

## Article

# Mechanical Activation of Smectite-Based Nanocomposites for Creation of Smart Fertilizers

Maxim Rudmin <sup>1,2,\*</sup> , Santanu Banerjee <sup>3</sup> , Boris Makarov <sup>4,5</sup>, Kanipa Ibraeva <sup>6</sup> and Alexander Konstantinov <sup>2</sup> 

<sup>1</sup> Division for Geology, Tomsk Polytechnic University, 634050 Tomsk, Russia

<sup>2</sup> Laboratory of Sedimentology and Paleobiosphere Evolution, University of Tyumen, 625003 Tyumen, Russia; konstantinov.alexandr72@gmail.com

<sup>3</sup> Department of Earth Sciences, Indian Institute of Technology Bombay, Mumbai 400076, India; santanu@iitb.ac.in

<sup>4</sup> Department of Plant Physiology and Biotechnology, Biological Institute, Tomsk State University, 634050 Tomsk, Russia; makar189@mail.ru

<sup>5</sup> Siberian Research Institute of Agriculture and Peat, Branch of the Siberian Federal Science Centre of Agrobiotechnologies, 634050 Tomsk, Russia

<sup>6</sup> School of Energy & Power Engineering, Tomsk Polytechnic University, 634050 Tomsk, Russia; kti1@tpu.ru

\* Correspondence: rudminma@tpu.ru; Tel.: +7-8-3822-60-62-45

**Abstract:** This research presents the mechanical creation of smart fertilizers from a mixture of smectite and urea in a 3:2 ratio by using the planetary milling technique. The smectite–urea composites show intercalation between urea and mineral, which increases steadily with increasing activation time. A shift of X-Ray Diffraction basal reflections, intensities of Fourier transform infrared spectroscopy (FTIR) peaks, and weight losses in thermogravimetric analysis (TG) document the systematic crystallochemical changes of the composites related to nitrogen interaction with activation. Observations of the nanocomposites by scanning electron microscopy (SEM) and transmission electron microscopy (TEM) corroborate the inference. Nitrogen intercalates with smectite in the interlayer space and remains absorbed either within micro-aggregates or on the surface of activated smectites. Soil leaching tests reveal a slower rate of nitrogen than that of traditional urea fertilizers. Different forms of nitrogen within the composites cause their differential release rates to the soil. The formulated nanocomposite fertilizer enhances the quality and quantity of oat yield.

**Keywords:** smectite; urea; fertilizer nanocomposite; mechanical activation; controlled release fertilizer; nitrogen fertilizer; polyfunctional fertilizer



**Citation:** Rudmin, M.; Banerjee, S.; Makarov, B.; Ibraeva, K.; Konstantinov, A. Mechanical Activation of Smectite-Based Nanocomposites for Creation of Smart Fertilizers. *Appl. Sci.* **2022**, *12*, 809. <https://doi.org/10.3390/app12020809>

Academic Editors: Claudio De Pasquale and Victoria Krupskaya

Received: 27 October 2021

Accepted: 12 January 2022

Published: 13 January 2022

**Publisher's Note:** MDPI stays neutral with regard to jurisdictional claims in published maps and institutional affiliations.



**Copyright:** © 2022 by the authors. Licensee MDPI, Basel, Switzerland. This article is an open access article distributed under the terms and conditions of the Creative Commons Attribution (CC BY) license (<https://creativecommons.org/licenses/by/4.0/>).

## 1. Introduction

Controlled-release fertilizers (CRF), or smart fertilizers [1], are essential for future, environment-friendly agronomic activities [2–9]. The agricultural productivity needs to increase to match the growing demand for food, as food requirement is expected to increase by 50% by 2050 [4,10,11]. Eco-friendly agronomic activities and waste-free crop production are crucial to sustain the demand. The application of traditional fertilizers causes adverse environmental consequences, although they increase the quality and quantity of crop [12]. The indiscriminate use of nitrogen fertilizers induces serious environmental problems, including nitrification, denitrification, downstream degradation of water quality, loss via runoff, volatilization, etc. [13,14]. The excess nutrients released by traditional fertilizers deteriorate subsurface and surface water [6,12,14–16]. The development of fertilizers with controlled nutrient release properties is a solution to this problem [5,6,17,18].

Several investigations were carried out in the past to assess the fertilizer potential using diverse materials, which include nanocomposites, such as polymers [3,19–23], clay minerals [23–27], or composites of synthetic and natural substances [28–32]. Compared to most synthetic products, clay minerals are cheap and easily available. Smectite

(montmorillonite), kaolinite, and, to a lesser extent, palygorskite or attapulgite, vermiculite, and chrysotile, as well as glauconite, are found to be potential CRFs [5,28,30,33–36].

The “green” fertilizers are formulated by choosing an inhibitor or substrate and nutrients appropriately [2,24,32–34,37–41]. Smectite is a useful “inhibitor” because of the high specific surface area caused by nano/micro-scale particles within it. The high surface charge and exchangeable structural sites (interlayer) in smectite facilitate nutrient exchange. Therefore, this geomaterial shows good sorption and ion-exchange properties [27,29,35,36,42]. It is used for “smart” fertilizer preparation by physical and mechanochemical methods involving dispersion and/or encapsulation techniques [21,40,43,44].

The goal of this work is to create effective and eco-friendly smart fertilizer by the activation of a smectite–urea mixture using the planetary mill, and to estimate the interaction between nitrogen and smectite. This study investigates different forms of nitrogen within the nanocomposites produced after the mechanical activation of initial mixtures and estimates the extent of intercalation, adsorbed, and absorbed nitrogen. Plant growth experiments were carried out to demonstrate the usefulness of CRFs on plant growth.

## 2. Materials and Methods

### 2.1. Minerals and Materials

This study uses smectite concentrate, the average formula of which is more as follows  $\text{Na}_{0.03-0.31}\text{Ca}_{0.06-0.13}(\text{Al}_{1.24-1.93}\text{Mg}_{0.19-0.36}\text{Fe}_{0.07-0.10})_{1.82-2.06}\text{Si}_{3.68-4.03}\text{Al}_{0.05-0.32}\text{O}_{10}(\text{OH})_{2n}\text{H}_2\text{O}$  [36].

The average formula of smectite was calculated based on energy-dispersive X-ray spectra (at least 50 analyses).

### 2.2. Mechanical Preparation of Composites

Initially, smectite (S) and urea (N) were mixed in the ratio of 3:2 (S3N2). The smectite–urea mixture was powdered under dry conditions by milling for different durations. The activation parameters were the following: an AGO-2 planetary mill, a rotation frequency of 1820 rpm, and a 1:5 ratio of powder to grinding bodies. The activation was conducted for each mixture (each weighing 20 g, which includes 12 g of smectite and 8 g of urea) for 3, 8, or 11 min to obtain three composites, named S3N2pm3, S3N2pm8, and S3N2pm11, respectively.

### 2.3. Analytical Study of Composites

Physical and chemical parameters of the composites were investigated using X-ray diffraction (XRD), scanning electron microscope attached with energy-dispersive X-ray spectroscopy (SEM-EDS), transmission electron microscopy (TEM), Fourier transform infrared spectroscopy (FTIR), and thermo-gravimetric analysis (TG). X-ray diffraction patterns of composites were obtained using a Bruker D2 Phase X-ray diffractometer (Billerica, MA, USA) by the following settings: Cu-K $\alpha$  radiation at a current of 10 mA, a voltage of 30 kV, 2-theta range ( $2\theta$ ) from 4° to 70°, a step size of 0.02° at a scanning rate of 1.5 s, divergence slit of 1 mm, the anti-scatter slit of 3 mm, and receiving slit of 0.3 mm. The composites were scanned by a scanning electron microscope of TESCAN VEGA 3 SBU (Brno, Czech Republic) with an OXFORD X-Max 50 adapter (High Wycombe, UK). Three composites were further scanned using a JEOL JEM-2100F (JEOL Ltd., Tokyo, Japan) transmission electron microscopy. A drop of a fine particle suspension was transferred to a copper grid (300 mesh, 3.05 mm in diameter) covered with a carbon film before TEM investigation at 200 kV. The infrared spectra of the samples were studied by using an FTIR spectrometer Shimadzu FTIR 8400S (Shimadzu, Kyoto, Japan) with the following parameters: a range from 4000 and 400  $\text{cm}^{-1}$ , and a resolution of 4  $\text{cm}^{-1}$ . Thermogravimetric analysis (TG) was conducted using an STA 449 F5 Jupiter micro-thermal analyzer (NETZSCH, Germany) by using the following conditions: a temperature diapason of 25–1000 °C, a heating rate of 10 K/min, and an inert argon atmosphere. The amount of intercalation between the urea and clay mineral was determined by the weight loss in the range of 300–580 °C.

#### 2.4. Soil Column Leaching Experiments

The nutrient release behavior of the smectite–urea composites was conducted by soil column leaching experiments [45–48]. Before testing, the total N content of each nanocomposite was determined by the Kjeldahl method. A bulk soil sample was collected from 0 to 20 cm deep surface layer from an experimental farm at Tomsk in Western Siberia. The soil was dried at room temperature after cleaning roots of plants and coarse materials (using a 2 mm sieve). The dry soil (80 g) was separately mixed with composites (65 mg) and traditional urea (39 mg) at a dose of  $380 \text{ mg N} \cdot \text{kg}^{-1}$  dry soil. Nitrogen content in composites was 30 mg. Care was given to make the mixture homogenous. The resultant mixture was taken into a PVC tube with a 100-mesh screen at the bottom (inner diameter 7 cm and height 25 cm). The bottom of the column was fitted with a Whatman filter paper #42. A PVC cap at the bottom of the column, with numerous small openings, prevented the loss of soil from the column. The surface of each soil column was covered with quartz sands to minimize the loss of volatiles. The experiment was carried out in a completely randomized design with five treatments, including three varieties of smectite–urea composites, with urea and one control devoid of composite/urea. Each treatment was repeated three times.

Throughout the experiment, the soil water content was maintained at 75% field capacity by weighing after 1, 4, 7, 14, 21, 28, 42, and 56 days. An amount of 200 mL of deionized water was added slowly into each soil column, and the leachates were collected in a 50 mL conical flask. Then, the leachates were filtered and stored at  $-24 \text{ }^\circ\text{C}$  for the chemical analyses. The potassium ( $\text{K}^+$ ), ammonium ( $\text{NH}_4^+$ ), and nitrate ( $\text{NO}_3^-$ ) contents, as well as the pH, were determined by AutoAnalyzer 3 (Bran Luebbe, Hamburg, Germany). Cumulative leaching amounts were calculated to evaluate the nitrogen release behavior of the prepared composites. The final values of cumulative leaching were determined by averages of three repetitions.

#### 2.5. Plant Growth Test

Germination experiments were carried out by using the composite S3N2-pm3/8/11. The untreated soil sample and the traditional urea fertilizer are, hereafter, referred to as the control samples. Oat (*Avena sativa*) seeds were germinated at room temperature ( $26 \pm 1 \text{ }^\circ\text{C}$ ) over 20 days on glass Petri dishes (9 cm diameter and 1.5 cm height). The composites and the urea were introduced into the soil at a concentration of 90 kg/ha. Each analysis was repeated three times. The soil used for this experiment was weakly acidic, agricultural dark grey, with 5.1 pH, and 4.1% of organic carbon. This soil is typical of S-E Western Siberia. The plants were watered every morning. Germination rate, seedling (plant) height, and dry weights of plants were measured. The germination rate is the ratio between the emergence number and the sown seed number. The germination rate was recorded daily in the first four days. The emergence amount was determined with plants having 2 cm of topsoil. The height and weight of oat plants were measured after harvesting (after 20 days). The oat seedlings were wrapped separately with paper sheets and kept in an oven (LF-25/350-GG1; JSC “Laboratory Equipment and Instruments” (LOIP), Saint Petersburg, Russia) at  $80 \text{ }^\circ\text{C}$ . As weights of seedling samples stabilized, their “dry weights” were measured.

#### 2.6. Statistical Analysis

Statistical analysis of results was carried out using Microsoft Excel 365. Values were calculated as arithmetic means with standard deviations. Means were performed by the least significant difference test at the 0.05 probability level.

### 3. Results

#### 3.1. Physical and Chemical Characteristics of Composites

The XRD patterns for the composites (Figure 1) show the prominent reflections of smectite (montmorillonite) at 14.3–17.3 and  $4.5 \text{ \AA}$ . The reflections at 4.0, 3.6, 3.1, 2.8, 2.5, 2.4, 2.2, 1.8, and  $1.7 \text{ \AA}$  confirm the presence of nitrogen. The reflections at 4.3 and  $3.4 \text{ \AA}$  correspond to quartz (4%) impurities in the smectite concentrate. The XRD patterns

also demonstrate the presence of illite and kaolinite (both up to 0.5%) at 10.0 and 7.1 Å, respectively. The basal reflection of smectite shifts from 14.3 to 17.3 Å (Figure 1) as the grinding time is increased from 3 min to 11 min.

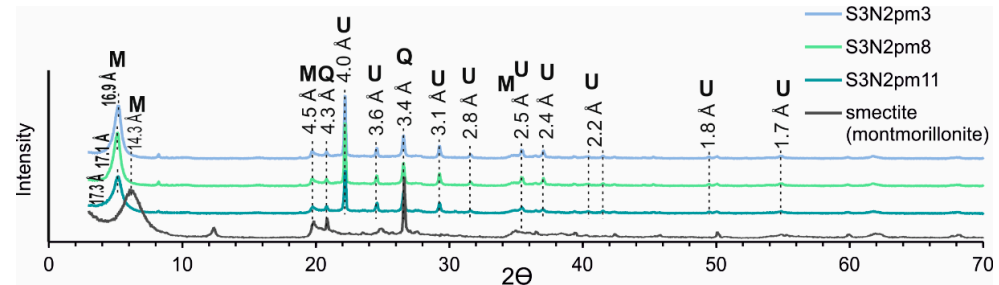


**Figure 1.** XRD patterns of the composites for different grinding times. Note the shift of smectite (M), urea (U) and quartz (Q) peaks in the composites.

The composite includes relics of smectite particles and flakes (Figure 2). A nitrogen coating mantles mineral micro-aggregates in S3N2pm11. The length of the mineral micro-aggregate's ranges from 10 to 200  $\mu\text{m}$ . The urea coating may be up to 5  $\mu\text{m}$  thick (Figure 2C). The urea coating thickens gradually as the operation time increases. The adsorbed urea crystallites within the coating have diameters ranging from 30 to 80 nm. They are admixed with nanoparticles of smectite (Figure 3). TEM images with SAED (Figure 3) show distinctive interplanar spacings for the following minerals: smectite of 17.1 Å and 4.5 Å; and urea of 3.6 Å, 3.1 Å, and 2.8 Å.

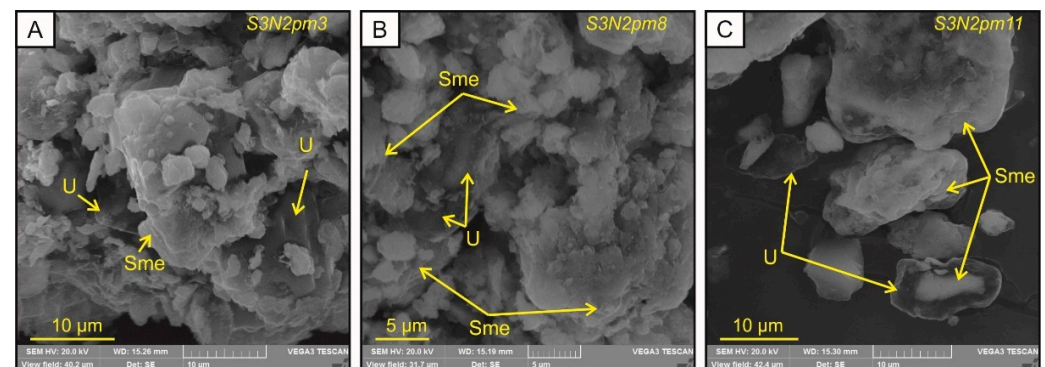


**Figure 2.** SEM images of composites S3N2pm3 (A), S3N2pm8 (B), and S3N2pm11 (C). Note the thicker urea coating in S3N2pm11 compared to other composites. U—urea particles, Sme—smectite (montmorillonite) relics.

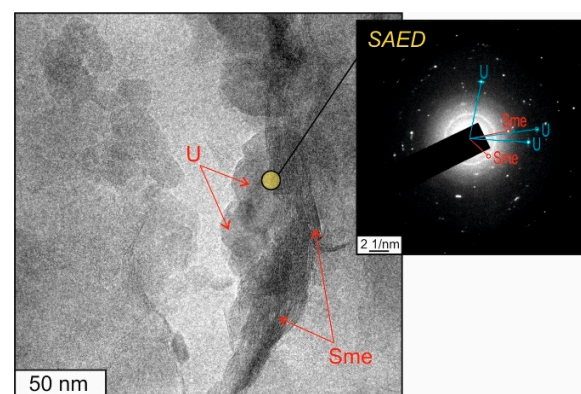


**Figure 3.** Transmission electron microscopy (TEM) images with selected area electron diffraction (SAED) patterns showing smectite (Sme) and urea (U) crystallite for S3N2pm11 composite.

The composites of S3N2pm3/8/11 (Figure 4) show minor changes of low wavenumber with increasing activation time. FTIR spectra of composites include peaks of CO at  $790\text{ cm}^{-1}$  and Si-O stretching at  $1050\text{ cm}^{-1}$ . All composites show a gentle peak at  $720\text{ cm}^{-1}$  ( $\text{NH}_2$ ). The  $\text{NH}_2$  peak is identified at  $1155\text{ cm}^{-1}$  in all the composites. Composites exhibit the asymmetric deformation of the C-N at  $1463\text{ cm}^{-1}$ . Peaks at  $1629\text{--}1650\text{ cm}^{-1}$  ( $\text{NH}_2$ ) and the flat  $1662\text{--}1683\text{ cm}^{-1}$  ( $\text{NH}$ ) are distinctive of the composites. These two peaks appear stronger in S3N2pm11 compared to S3N2pm 3/8. FTIR peaks of S3N2pm11 characteristically exhibit a peak at  $3344\text{ cm}^{-1}$ , probably reflecting the nitrogen coating. The  $\text{NH}_2$  peak shifts from  $3485$  to  $3440\text{ cm}^{-1}$  with increasing grinding time. All composites show a peak of  $3620\text{ cm}^{-1}$ , which is associated with IR-vibration Al-OH-Al of montmorillonite.

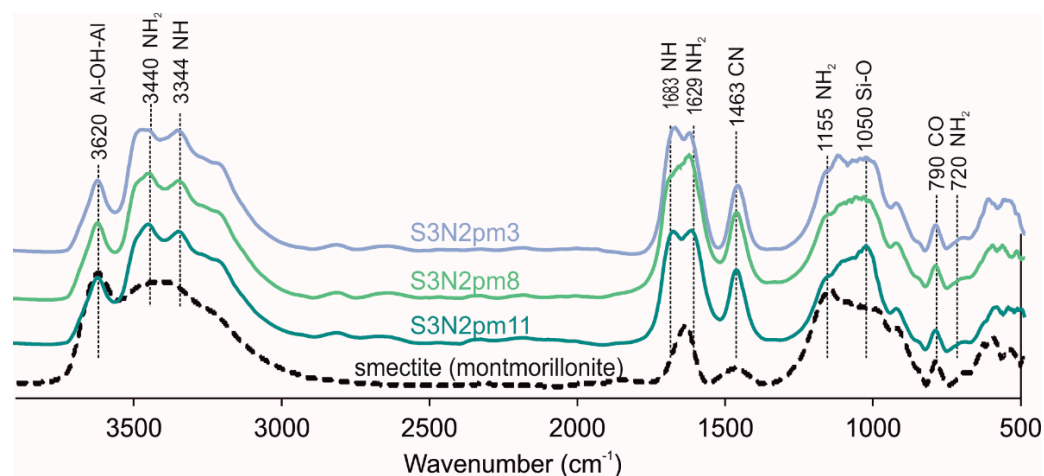


**Figure 4.** FTIR spectra of the S3N2pm composites. Note the systematic shifts in spectral characteristics of composites with increasing grinding time compared to smectite (montmorillonite).

The composites are characterized by six weight loss steps on the thermogravimetric (TG) curves:  $0\text{--}135\text{ }^{\circ}\text{C}$ ,  $135\text{--}240\text{ }^{\circ}\text{C}$ ,  $240\text{--}300\text{ }^{\circ}\text{C}$ ,  $300\text{--}450\text{ }^{\circ}\text{C}$ ,  $450\text{--}580\text{ }^{\circ}\text{C}$ , and  $580\text{--}1000\text{ }^{\circ}\text{C}$  (Figure 5, Table 1). The curves of composites exhibit weight losses by 0.8–1.1% and 20.4–21.0% in the steps of  $0\text{--}135\text{ }^{\circ}\text{C}$  and  $135\text{--}240\text{ }^{\circ}\text{C}$ , because of the release of free water and adsorbed urea, respectively [49,50]. The third and fourth weight loss steps at  $240\text{--}300\text{ }^{\circ}\text{C}$  and  $300\text{--}450\text{ }^{\circ}\text{C}$  indicate the decomposition of absorbed and intercalated urea, respectively [39,51]. The absorbed urea (within smectite micro-aggregates) is removed by weight losses of 3.2–3.7% (equal to 8–9.2% of used urea) in a weight loss range of  $240\text{--}300\text{ }^{\circ}\text{C}$ . Part of the intercalated urea is lost by 12.9–13.6% in a step of  $300\text{--}450\text{ }^{\circ}\text{C}$ . The fifth step at the temperature range of  $450\text{--}590\text{ }^{\circ}\text{C}$  corresponds to the removal of intercalated urea [52] by 4.1–4.9% from the composites. In general, the intercalated urea in composites becomes 17.0–18.4%, equal to 42.5–46.0% of used urea. The temperature interval  $590\text{--}1000\text{ }^{\circ}\text{C}$  (the six weight loss step) corresponds to the dehydroxylation of mineral [53] by 2.0–3.1%. The maximum nitrogen intercalation into the smectite was obtained for a grinding time of 11 min.

**Table 1.** The weight losses (%) of smectite–urea composites according to TG curves.

Weight Loss Steps, $^{\circ}\text{C}$	S3N2pm3	S3N2pm8	S3N2pm11
0–135	0.8	1.0	1.1
135–240	20.4	21.0	20.9
240–300	3.2	3.6	3.7
300–450	12.9	13.6	13.5
450–580	4.1	4.3	4.9
580–1000	3.1	2.1	2.0

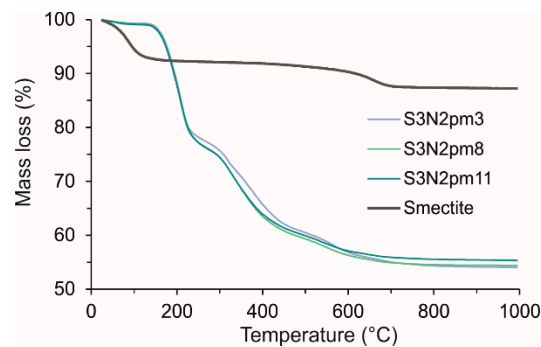


**Figure 5.** TG patterns of smectite–urea composites compared with smectite. The weight losses of the intercalated nitrogen in intervals of 300–450 °C and 450–590 °C.

### 3.2. Nutrient Release Characteristics of Composites

The release of nitrogen from the composites was studied by the soil column leaching experiment (Figure 6). The release of ammonium ( $\text{NH}_4^+$ ) from the composites was faster in the first 7 days than in the remaining period (Figure 6A). The ammonium content in the leached solution was almost similar in the first few days for all composites. After the first week, the composite S3N2pm11 released higher  $\text{NH}_4^+$  relative to others. The leaching rate of ammonium was stable after the 28th day for all samples, which was followed by the overlapping leaching curves (Figure 6A). The urea control released ammonium at the fastest rate at each stage of the experiment. The release of nitrates took place at different rates during the experiment (Figure 6B). The nitrate was leached in four steps, namely: up to the 7th day, from the 7th to 21st day, from the 21st to 28th day, and from the 28th to 56th day. However, the urea control released the most nitrate at all stages. The composite S3N2pm11 released nitrate at the slowest rate. The rate of release of nitrate stabilized after the 28th day for all samples. The total nitrogen was released in four stages, following the similar fashion of nitrate release (Figure 6C).

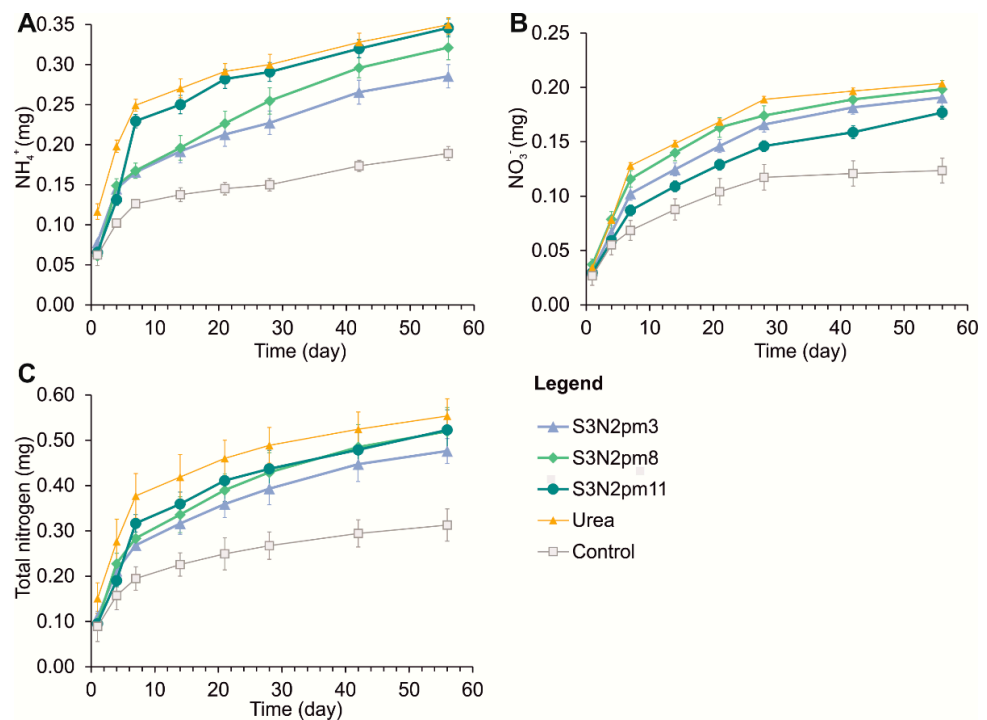


**Figure 6.** Cumulative release of (A)  $\text{NH}_4^+$ , (B)  $\text{NO}_3^-$ , and (C) total nitrogen during the soil leaching test. Note the sharp decrease in the steepness of curves after 6 to 7 days. The statistical significance of every parameter indicates at the  $p = 0.05$  level. Bars represent standard deviation.

### 3.3. Application of Composites for Plant Growth

The germination rate of the plant (Figure 7A) varied from 92.0% to 95.9% for plots with the composites. The germination rate increased by 5.2% compared to the control while using the S3N2pm11 composite. In comparison, the germination rate increased by 6.6% in the case of urea relative to the control. The average height of seedlings increased more with the application of the composites compared to the control (Figure 7B). The composite showed an increase in plant height ranging from 3.0% to 7.3% relative to the control sample. The S3N2pm11 composite recorded the maximum increase. The rate of increase of dry weight (Figure 7C) of plants was higher in the case of composites and urea than the control soil. The urea showed the maximum increase of dry weight. The dry weight recorded 6.1% more increase in the composite S3N2pm11 than the control. The composite S3N2pm11 and the urea showed higher growth of seedling weight than others (Figure 7).

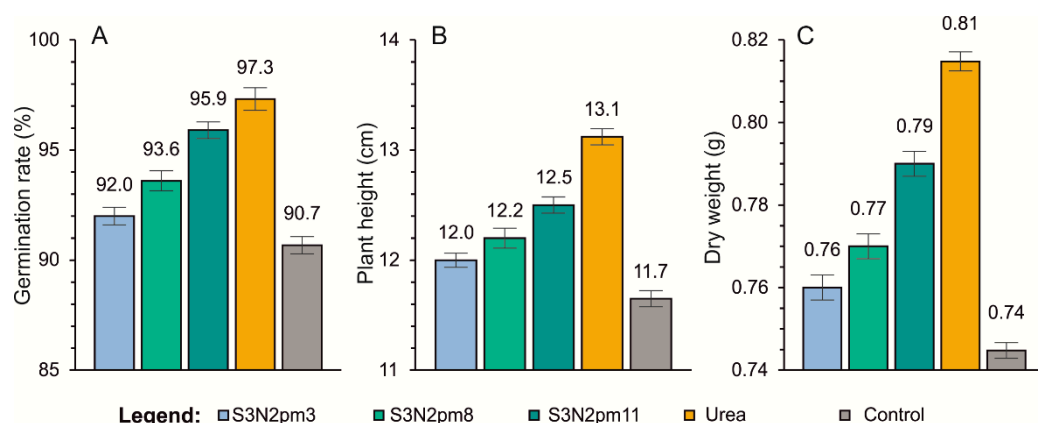


**Figure 7.** Histograms showing the % increase of (A)—germination rate, (B)—seedling height, and (C)—dry weight of oat (*Avéna satíva*). Note that urea and composites are equally effective fertilizers for plant growth. Further note that the composite S3N2pm11 is the most effective for plant growth as it records the maximum increase of all three parameters. The statistical significance of every parameter indicates at the  $p = 0.05$  level. Bars represent standard deviation.

## 4. Discussion

### 4.1. Nanocomposites Made up of Smectite and Urea Mixture

The creation of clay-based smart fertilizer is performed using different approaches, including milling [24,33,34,41], aqueous suspension technique [29], premixing the components, followed by extrusion and drying [52,54], mixing of bentonite and liquefied urea [55], and using irradiation method [35]. The previous mechanochemical activation tests were conducted with a mixture of smectite and urea in a 2:3 ratio [36]. It led to the creation of composites with different forms of nitrogen. This research focuses on new ratios of substances in composite products and an optimal activation time in planetary milling and on the variable rates of release of nitrogen depending on the interrelationship between smectite and urea in the composites. Three types of interrelationships between smectite and urea, which were observed by morphology and structure of composites (Figures 1–5), are as follows: (i) nitrogen intercalations in the interlayer space of smectite, (ii) nitrogen absorption into the micropores of smectites, and (iii) adsorption of nitrogen as films covering micro-aggregates of smectite.

The planetary milling activation of a smectite and urea mixture in a ratio of 3:2 leads to the formation of controlled release fertilizer nanocomposites. The intercalated urea increases from 17.0 to 18.4% as the grinding time is increased from 3 min to 11 min. The external coating of micro-aggregates thickens by 20.4–21.0% as the duration of milling increases (Figure 2C).

The shift of the basal reflection to higher  $d$ -values with increased activation duration corresponds to increased nitrogen in the interlayer mineral space (Figure 1). The shift of 001 reflection indicates the replacement of solvating cations by urea in activated composites

(Figures 1 and 3), recorded by the absence of the weight loss of solvating water from smectite. Composites are characterized by the shift of the basal reflection from 14.3 to 17.3 Å, indicating the presence of nitrogen within the smectite structure. The nitrogen remains absorbed within the isometric microcrystallites (up to 80 nm long) within the smectite (Figure 3).

The intensity of  $\text{NH}_2$  at  $1155\text{ cm}^{-1}$  increased by enhanced operation time, related to the adsorption of nitrogen on smectite flakes (Figure 4). The  $\text{NH}_2$  peak changed from  $3485\text{ cm}^{-1}$  to  $3440\text{ cm}^{-1}$  with increased activation time, suggesting intercalation of nitrogen molecules. The shifts of  $\text{NH}_2$  and  $\text{NH}$  peaks indicate the gradual intercalation of these molecules into the interlayer space of smectite (Figure 4) with increasing activation time.

#### 4.2. Usefulness of Composites as Smart Fertilizers

The results of this research are comparable with the data obtained by the mechanochemical activation of smectite [29,55–57], glauconite [27,36,58], palygorskite [19,59], and kaolinite [39,40,60] for application as modern polyfunctional fertilizers. Nitrogen is released from the composites at different rates for the duration of the experiments (Figure 6), which is probably due to various forms of nitrogen. The external coating releases the nitrogen at the initial stage while the absorbed nitrogen is released at the next stage, after 21 days of soil leaching experiment. The intercalated portion releases nutrients at the final stage.

The introduction of the composites within weakly acidic soil boosts the seeding and growth of oat (*Avena sativa*). The S3N2pm11 composite is found to be the most effective for promoting plant growth (Figure 7). The S3N2pm11 composite and traditional urea show comparable effectiveness regarding crop production (dry weight and plant height). Therefore, composite fertilizers, based on smectite and urea mixture, are an alternative to traditional urea. The ability of the composites to release nutrients slowly makes it an environment-friendly option for composite fertilizer. Moreover, the smectite–urea composites are controlled-release fertilizers. Future studies need to include suitable and eco-friendly minerals with macro- and micronutrients and cost-effective techniques for CRF.

## 5. Conclusions

Mineral-based composites with controlled-release properties were formulated by the mechanical activation of smectite and urea mixture in a ratio of 3:2. The composites showed the different interrelationships between smectite and nitrogen. The nitrogen may remain intercalated in mineral interlayer space and absorbed either in the pores between micro-aggregates or on the surface of activated mineral particles. The composites boost plant growth effectively. Due to the controlled release of nitrogen, the composites are considered as smart fertilizers. Soil leaching tests confirm the slow release of nitrogen compared to traditional fertilizers. Therefore, activated composites are polyfunctional fertilizers. The composites support the growth of oat, similar to traditional urea fertilizer.

**Author Contributions:** Conceptualization, M.R.; methodology, M.R. and B.M.; investigation, M.R., S.B., B.M., K.I. and A.K.; resources, M.R.; data curation, M.R. and B.M.; writing—original draft preparation, M.R., S.B. and A.K.; writing—review and editing, M.R. and S.B.; visualization, M.R.; project administration, M.R.; funding acquisition, M.R. All authors have read and agreed to the published version of the manuscript.

**Funding:** This study was supported by a grant from the President of the Russian Federation to support young Russian scientists, project number MK-213.2020.5.

**Institutional Review Board Statement:** Not applicable.

**Informed Consent Statement:** Not applicable.

**Data Availability Statement:** Not applicable.

**Acknowledgments:** M.R. and A.K. acknowledge support from the Ministry of Science and Higher Education of the Russian Federation (project FEWZ-2020-0007) and the Center for Collective Use “Bioinert Systems of the Cryosphere” (Tyumen Scientific Center, SB RAS).

**Conflicts of Interest:** The authors declare no conflict of interest.

## References

- Raimondi, G.; Maucieri, C.; Toffanin, A.; Renella, G.; Borin, M. Smart fertilizers: What should we mean and where should we go? *Ital. J. Agron.* **2021**, *16*, 1794. [[CrossRef](#)]
- Lawrencina, D.; Wong, S.K.; Low, D.Y.S.; Goh, B.H.; Goh, J.K.; Ruktanonchai, U.R.; Soottitantawat, A.; Lee, L.H.; Tang, S.Y. Controlled Release Fertilizers: A Review on Coating Materials and Mechanism of Release. *Plants* **2021**, *10*, 238. [[CrossRef](#)] [[PubMed](#)]
- Gu, H.; Geng, H.; Wang, D.; Li, W. A new method for the treatment of kitchen waste: Converting it into agronomic sprayable mulch film. *Waste Manag.* **2021**, *126*, 527–535. [[CrossRef](#)] [[PubMed](#)]
- Rahman, M.H.; Haque, K.M.S.; Khan, M.Z.H. A review on application of controlled released fertilizers influencing the sustainable agricultural production: A Cleaner production process. *Environ. Technol. Innov.* **2021**, *23*, 101697. [[CrossRef](#)]
- Sikora, J.; Niemiec, M.; Szeląg-Sikora, A.; Gródek-Szostak, Z.; Kuboń, M.; Komorowska, M. The Impact of a Controlled-Release Fertilizer on Greenhouse Gas Emissions and the Efficiency of the Production of Chinese Cabbage. *Energies* **2020**, *13*, 2063. [[CrossRef](#)]
- Vakal, S.; Yanovska, A.; Vakal, V.; Artyukhov, A.; Shkola, V.; Yarova, T.; Dmitrikov, V.; Krmela, J.; Malovanyy, M. Minimization of Soil Pollution as a Result of the Use of Encapsulated Mineral Fertilizers. *J. Ecol. Eng.* **2020**, *22*, 221–230. [[CrossRef](#)]
- Wei, H.; Chen, Z.; Xing, Z.; Zhou, L.; Liu, Q.; Zhang, Z.; Jiang, Y.; Hu, Y.; Zhu, J.; Cui, P.; et al. Effects of slow or controlled release fertilizer types and fertilization modes on yield and quality of rice. *J. Integr. Agric.* **2018**, *17*, 2222–2234. [[CrossRef](#)]
- Trenkel, M.E. *Slow- and Controlled-Release and Stabilized Fertilizers: An Option for Enhancing Nutrient Use Efficiency in Agriculture*; International Fertilizer Industry Association (IFA): Paris, France, 2010; ISBN 9788578110796.
- Vejan, P.; Khadiran, T.; Abdullah, R.; Ahmad, N. Controlled release fertilizer: A review on developments, applications and potential in agriculture. *J. Control. Release* **2021**, *339*, 321–334. [[CrossRef](#)]
- Tilman, D.; Cassman, K.G.; Matson, P.A.; Naylor, R.; Polasky, S. Agricultural sustainability and intensive production practices. *Nature* **2002**, *418*, 671–677. [[CrossRef](#)] [[PubMed](#)]
- Pretty, J.; Sutherland, W.J.; Ashby, J.; Auburn, J.; Baulcombe, D.; Bell, M.; Bentley, J.; Bickersteth, S.; Brown, K.; Burke, J.; et al. The top 100 questions of importance to the future of global agriculture. *Int. J. Agric. Sustain.* **2010**, *8*, 219–236. [[CrossRef](#)]
- Xiao, Y.; Peng, F.; Zhang, Y.; Wang, J.; Zhuge, Y.; Zhang, S.; Gao, H. Effect of bag-controlled release fertilizer on nitrogen loss, greenhouse gas emissions, and nitrogen applied amount in peach production. *J. Clean. Prod.* **2019**, *234*, 258–274. [[CrossRef](#)]
- Vitousek, P.M.; Naylor, R.; Crews, T.; David, M.B.; Drinkwater, L.E.; Holland, E.; Johnes, P.J.; Katzenberger, J.; Martinelli, L.A.; Matson, P.A.; et al. Nutrient imbalances in agricultural development. *Science* **2009**, *324*, 1519–1520. [[CrossRef](#)]
- Akiyama, H.; Yan, X.; Yagi, K. Evaluation of effectiveness of enhanced-efficiency fertilizers as mitigation options for N<sub>2</sub>O and NO emissions from agricultural soils: Meta-analysis. *Glob. Chang. Biol.* **2010**, *16*, 1837–1846. [[CrossRef](#)]
- Ju, X.-T.; Xing, G.-X.; Chen, X.-P.; Zhang, S.-L.; Zhang, L.-J.; Liu, X.-J.; Cui, Z.-L.; Yin, B.; Christie, P.; Zhu, Z.-L.; et al. Reducing environmental risk by improving N management in intensive Chinese agricultural systems. *Proc. Natl. Acad. Sci. USA* **2009**, *106*, 3041–3046. [[CrossRef](#)]
- Zhang, Z.S.; Chen, J.; Liu, T.Q.; Cao, C.G.; Li, C.F. Effects of nitrogen fertilizer sources and tillage practices on greenhouse gas emissions in paddy fields of central China. *Atmos. Environ.* **2016**, *144*, 274–281. [[CrossRef](#)]
- Goulding, K.; Jarvis, S.; Whitmore, A. Optimizing nutrient management for farm systems. *Philos. Trans. R. Soc. B: Biol. Sci.* **2008**, *363*, 667–680. [[CrossRef](#)]
- Sha, Z.; Lv, T.; Staal, M.; Ma, X.; Wen, Z.; Li, Q.; Pasda, G.; Misselbrook, T.; Liu, X. Effect of combining urea fertilizer with P and K fertilizers on the efficacy of urease inhibitors under different storage conditions. *J. Soils Sediments* **2020**, *20*, 2130–2140. [[CrossRef](#)]
- Ni, B.; Liu, M.; Lü, S.; Xie, L.; Wang, Y. Environmentally Friendly Slow-Release Nitrogen Fertilizer. *J. Agric. Food Chem.* **2011**, *59*, 10169–10175. [[CrossRef](#)]
- Qiao, D.; Liu, H.; Yu, L.; Bao, X.; Simon, G.P.; Petinakis, E.; Chen, L. Preparation and characterization of slow-release fertilizer encapsulated by starch-based superabsorbent polymer. *Carbohydr. Polym.* **2016**, *147*, 146–154. [[CrossRef](#)] [[PubMed](#)]
- Wu, L.; Liu, M. Preparation and properties of chitosan-coated NPK compound fertilizer with controlled-release and water-retention. *Carbohydr. Polym.* **2008**, *72*, 240–247. [[CrossRef](#)]
- Rashid, M.; Hussain, Q.; Khan, K.S.; Alwabel, M.I.; Hayat, R.; Akmal, M.; Ijaz, S.S.; Alvi, S.; Obaid-ur-Rehman. Carbon-Based Slow-Release Fertilizers for Efficient Nutrient Management: Synthesis, Applications, and Future Research Needs. *J. Soil Sci. Plant Nutr.* **2021**, *21*, 1144–1169. [[CrossRef](#)]
- Pereira, E.I.; da Cruz, C.C.T.; Solomon, A.; Le, A.; Cavigelli, M.A.; Ribeiro, C. Novel Slow-Release Nanocomposite Nitrogen Fertilizers: The Impact of Polymers on Nanocomposite Properties and Function. *Ind. Eng. Chem. Res.* **2015**, *54*, 3717–3725. [[CrossRef](#)]

24. Borges, R.; Brunatto, S.F.; Leitão, A.A.; De Carvalho, G.S.G.; Wypych, F. Solid-state mechanochemical activation of clay minerals and soluble phosphate mixtures to obtain slow-release fertilizers. *Clay Miner.* **2015**, *50*, 153–162. [[CrossRef](#)]
25. Lei, Z.; Cagnetta, G.; Li, X.; Qu, J.; Li, Z.; Zhang, Q.; Huang, J. Enhanced adsorption of potassium nitrate with potassium cation on H<sub>3</sub>PO<sub>4</sub> modified kaolinite and nitrate anion into Mg-Al layered double hydroxide. *Appl. Clay Sci.* **2018**, *154*, 10–16. [[CrossRef](#)]
26. Solihin, Z.Q.; Tongamp, W.; Saito, F. Mechanochemical synthesis of kaolin–KH<sub>2</sub>PO<sub>4</sub> and kaolin–NH<sub>4</sub>H<sub>2</sub>PO<sub>4</sub> complexes for application as slow release fertilizer. *Powder Technol.* **2011**, *212*, 354–358. [[CrossRef](#)]
27. Rudmin, M.; Abdullayev, E.; Ruban, A.; Buyakov, A.; Soktoev, B. Mechanochemical Preparation of Slow Release Fertilizer Based on Glauconite–Urea Complexes. *Minerals* **2019**, *9*, 507. [[CrossRef](#)]
28. Atia, A.A.; Donia, A.M.; Hussin, R.A.; Rashad, R.T. Swelling and metal ion uptake characteristics of kaolinite containing poly [(acrylic acid)-co-acrylamide] hydrogels. *Desalination Water Treat.* **2009**, *3*, 73–82. [[CrossRef](#)]
29. Golbashy, M.; Sabahi, H.; Allahdadi, I.; Nazokdast, H.; Hosseini, M. Synthesis of highly intercalated urea-clay nanocomposite via domestic montmorillonite as eco-friendly slow-release fertilizer. *Arch. Agron. Soil Sci.* **2017**, *63*, 84–95. [[CrossRef](#)]
30. Rashidzadeh, A.; Olad, A. Slow-released NPK fertilizer encapsulated by NaAlg-g-poly (AA-co-AAm)/MMT superabsorbent nanocomposite. *Carbohydr. Polym.* **2014**, *114*, 269–278. [[CrossRef](#)]
31. Pimsen, R.; Porrawatukul, P.; Nuengmatcha, P.; Ramasoot, S.; Chanthai, S. Efficiency enhancement of slow release of fertilizer using nanozeolite–chitosan/sago starch-based biopolymer composite. *J. Coat. Technol. Res.* **2021**, *18*, 1321–1332. [[CrossRef](#)]
32. de Oliveira, D.S.; Jaerger, S.; Marangoni, R. Mechanochemical synthesis of expanded vermiculite with urea for filler into alginate/collagen spherical capsules: A urea slow-release system. *Orbital* **2021**, *13*, 124–130. [[CrossRef](#)]
33. Borges, R.; Prevot, V.; Forano, C.; Wypych, F. Design and Kinetic Study of Sustainable Potential Slow-Release Fertilizer Obtained by Mechanochemical Activation of Clay Minerals and Potassium Monohydrogen Phosphate. *Ind. Eng. Chem. Res.* **2017**, *56*, 708–716. [[CrossRef](#)]
34. Borges, R.; Wypych, F. Potential slow release fertilizers and acid soil conditioners obtained by one-pot mechanochemical activation of chrysotile: Cement roofing sheets with K<sub>2</sub>/HPO<sub>4</sub>. *J. Braz. Chem. Soc.* **2019**, *30*, 326–332.
35. Fatimah, I.; Yudha, S.P.; Rubiyanto, D.; Widodo, I.D. Methenamine-smectite clay as slow release fertiliser: Physicochemical and kinetics study. *Chem. Eng. Trans.* **2017**, *56*, 1639–1644.
36. Rudmin, M.; Banerjee, S.; Yakich, T.; Tabakaev, R.; Ibraeva, K.; Buyakov, A.; Soktoev, B.; Ruban, A. Formulation of a slow-release fertilizer by mechanical activation of smectite/glauconite and urea mixtures. *Appl. Clay Sci.* **2020**, *196*, 105775. [[CrossRef](#)]
37. Beig, B.; Niazi, M.B.K.; Jahan, Z.; Hussain, A.; Zia, M.H.; Mehran, M.T. Coating materials for slow release of nitrogen from urea fertilizer: A review. *J. Plant Nutr.* **2020**, *43*, 1510–1533. [[CrossRef](#)]
38. Fu, J.; Wang, C.; Chen, X.; Huang, Z.; Chen, D. Classification research and types of slow controlled release fertilizers (SRFs) used—A review. *Commun. Soil Sci. Plant Anal.* **2018**, *49*, 2219–2230. [[CrossRef](#)]
39. Makó, É.; Kristóf, J.; Horváth, E.; Vágvolgyi, V. Kaolinite-urea complexes obtained by mechanochemical and aqueous suspension techniques—A comparative study. *J. Colloid Interface Sci.* **2009**, *330*, 367–373. [[CrossRef](#)]
40. Rutkai, G.; Makó, É.; Kristóf, T. Simulation and experimental study of intercalation of urea in kaolinite. *J. Colloid Interface Sci.* **2009**, *334*, 65–69. [[CrossRef](#)]
41. Borges, R.; Baika, L.M.; Grassi, M.T.; Wypych, F. Mechanochemical conversion of chrysotile/K<sub>2</sub>HPO<sub>4</sub> mixtures into potential sustainable and environmentally friendly slow-release fertilizers. *J. Environ. Manag.* **2018**, *206*, 962–970. [[CrossRef](#)]
42. Puspita, A.; Pratiwi, G.; Fatimah, I. Chitosan-modified smectite clay and study on adsorption-desorption of urea. *Chem. Eng. Trans.* **2017**, *56*, 1645–1650.
43. Liang, R.; Liu, M.; Wu, L. Controlled release NPK compound fertilizer with the function of water retention. *React. Funct. Polym.* **2007**, *67*, 769–779. [[CrossRef](#)]
44. Sharma, G.C. Controlled-release fertilizers and horticultural applications. *Sci. Hortic.* **1979**, *11*, 107–129. [[CrossRef](#)]
45. Yamamoto, C.F.; Pereira, E.I.; Mattoso, L.H.C.; Matsunaka, T.; Ribeiro, C. Slow release fertilizers based on urea/urea–formaldehyde polymer nanocomposites. *Chem. Eng. J.* **2016**, *287*, 390–397. [[CrossRef](#)]
46. Chen, S.; Yang, M.; Ba, C.; Yu, S.; Jiang, Y.; Zou, H.; Zhang, Y. Preparation and characterization of slow-release fertilizer encapsulated by biochar-based waterborne copolymers. *Sci. Total Environ.* **2018**, *615*, 431–437. [[CrossRef](#)]
47. González, M.E.; Cea, M.; Medina, J.; González, A.; Diez, M.C.; Cartes, P.; Monreal, C.; Navia, R. Evaluation of biodegradable polymers as encapsulating agents for the development of a urea controlled-release fertilizer using biochar as support material. *Sci. Total Environ.* **2015**, *505*, 446–453. [[CrossRef](#)]
48. Jiao, G.-J.; Peng, P.; Sun, S.-L.; Geng, Z.-C.; She, D. Amination of biorefinery technical lignin by Mannich reaction for preparing highly efficient nitrogen fertilizer. *Int. J. Biol. Macromol.* **2019**, *127*, 544–554. [[CrossRef](#)]
49. Schaber, P.M.; Colson, J.; Higgins, S.; Thielen, D.; Anspach, B.; Brauer, J. Thermal decomposition (pyrolysis) of urea in an open reaction vessel. *Thermochim. Acta* **2004**, *424*, 131–142. [[CrossRef](#)]
50. Chi, Y.; Zhang, G.; Xiang, Y.; Cai, D.; Wu, Z. Fabrication of reusable temperature-controlled-released fertilizer using a palygorskite-based magnetic nanocomposite. *Appl. Clay Sci.* **2018**, *161*, 194–202. [[CrossRef](#)]
51. Kristóf, J.; Frost, R.L.; Horváth, E.; Kocsis, L.; Inczédy, J. Thermoanalytical investigations on intercalated kaolinites. *J. Therm. Anal. Calorim.* **1998**, *53*, 467–475. [[CrossRef](#)]

52. Pereira, E.I.; Nogueira, A.R.A.; Cruz, C.C.T.; Guimarães, G.G.F.; Foschini, M.M.; Bernardi, A.C.C.; Ribeiro, C. Controlled Urea Release Employing Nanocomposites Increases the Efficiency of Nitrogen Use by Forage. *ACS Sustain. Chem. Eng.* **2017**, *5*, 9993–10001. [[CrossRef](#)]
53. Emmerich, K.; Madsen, F.T.; Kahr, G. Dehydroxylation behavior of heat-treated and steam-treated homoionic cis-vacant montmorillonites. *Clays Clay Miner.* **1999**, *47*, 591–604. [[CrossRef](#)]
54. Gu, H.; Zhang, Y.; Li, X.; Li, W.; Huang, S. Lignin improves release behavior of slow-release fertilizers with high content of urea. *J. Appl. Polym. Sci.* **2019**, *10*, 48238. [[CrossRef](#)]
55. Hermida, L.; Agustian, J. Slow release urea fertilizer synthesized through recrystallization of urea incorporating natural bentonite using various binders. *Environ. Technol. Innov.* **2019**, *13*, 113–121. [[CrossRef](#)]
56. Abramova, E.; Lapidés, I.; Yariv, S. Thermo-XRD investigation of monoionic montmorillonites mechanochemically treated with urea. *J. Therm. Anal. Calorim.* **2007**, *90*, 99–106. [[CrossRef](#)]
57. Rudmin, M.A.; Reva, I.V.; Yakich, T.Y.; Soktoev, B.R.; Buyakov, A.S.; Tabakaev, R.B.; Ibraeva, K. Montmorillonite as a prospective composite mineral for the creation of modern slow-release fertilizers. *Bull. Tomsk Polytech. Univ. Geo Assets Eng.* **2021**, *332*, 14–22.
58. Singla, R.; Alex, T.C.; Kumar, R. On mechanical activation of glauconite: Physicochemical changes, alterations in cation exchange capacity and mechanisms. *Powder Technol.* **2020**, *360*, 337–351. [[CrossRef](#)]
59. Liang, R.; Liu, M. Preparation and Properties of Coated Nitrogen Fertilizer with Slow Release and Water Retention. *Ind. Eng. Chem. Res.* **2006**, *45*, 8610–8616. [[CrossRef](#)]
60. Al-Rawajfeh, A.E.; AlShamaileh, E.M.; Alrbaihat, M.R. Clean and efficient synthesis using mechanochemistry: Preparation of kaolinite–KH<sub>2</sub>PO<sub>4</sub> and kaolinite–(NH<sub>4</sub>)<sub>2</sub>HPO<sub>4</sub> complexes as slow released fertilizer. *J. Ind. Eng. Chem.* **2019**, *73*, 336–343. [[CrossRef](#)]